International Conference on Space Optics—ICSO 2018

Chania, Greece

9–12 October 2018

Characterisation and performance verification results of the EarthCARE multi spectral imager VNS camera

Bryan T. de Goeij

Dick de Bruijn

Frits van der Knaap

Hans Bol

et al.

Characterisation and Performance Verification Results of the EarthCARE Multi Spectral Imager VNS Camera

Bryan T.G. de Goeij*[a], Dick de Bruijn[a], Frits van der Knaap[a], Hans Bol[a], Wim Gielesen[a], Andrew Bell[a], Alan Matthews[b], Mark Skipper[b], Ben Hallett[b], Maximilian Sauer[c], Klaus-Werner Kruse[c], Cornelius Haas[c], Kotska Wallace[d], Arnaud Heliere[d]

[a] TNO, Delft, The Netherlands; [b] Surrey Satellite Technology Ltd., Guildford, UK; [c] Airbus Defence and Space GmbH, Friedrichshafen, Germany; [d] European Space Agency, Noordwijk, The Netherlands

ABSTRACT

The European Space Agency (ESA) and the Japan Aerospace Exploration Agency (JAXA) are co-operating to develop the EarthCARE satellite mission with the fundamental objective of improving the understanding of the processes involving clouds, aerosols and radiation in the Earth's atmosphere.

A Cloud Profiling Radar (CPR), an Atmospheric LIDAR (ATLID), a Broadband Radiometer (BBR) and a Multi-Spectral Imager (MSI) constitute the payload complement of the EarthCARE satellite. The four instruments will provide synergistic data on cloud and aerosol vertical structure, horizontal cloud structure and radiant flux from sub-satellite cells. By acquiring images of the clouds and aerosol distribution, the MSI instrument will provide important contextual information in support of the radar and LIDAR data processing.

The MSI instrument itself consists of two camera units, the Thermal Infrared (TIR) camera and the Visible, Near-Infrared and Shortwave Infrared (VNS) camera, that are readout through a shared Front-End-Electronics (FEE) unit, all controlled by the Instrument Control unit (ICU).

The subject of this paper is the characterisation and performance verification results of the TNO designed and built Proto Flight Model (PFM) VNS camera in conjunction with the SSTL designed and built PFM FEE unit. This paper presents an overview of the characterisation and performance verification philosophy, followed by a more detailed presentation of several important measurements sets highlighted below.

Optical quality measurements (Modulation Transfer Function)
In order to measure the MTF of the VNS camera for several spatial frequencies simultaneously, a dedicated laboratory setup was built that provided the camera with block illumination patterns. Using Fourier analysis these optical block functions could be separated into their higher order components, resulting in acquisition of the MTF performance for several spatial frequencies concurrently.

Spectral Response measurements
For the VNS camera the spectral response was measured from 300nm up to 2400nm over the entire instrument swath of 360pixels. In order to perform this in an efficient manner a lock-in amplification setup was devised that included a "high" power pulsed tunable laser source, integrating spheres and monitoring detector.

In order to control pulse to pulse variations of the laser source and have a correct background correction, the 1kHz pulse frequency of the laser was further modulated by a several Hz chopper, resulting in spectral measurements with ~1% accuracy.

Straylight measurements
The straylight requirements for the VNS camera were specified as the maximum allowable amount of signal in an infinite dark area when illuminating the VNS camera with semi- infinite light source in an adjacent area. A dedicated tool was developed to simulate these (semi) infinite areas.

Radiometric characterization
For the VNS camera the required absolute radiometric accuracy was quite relaxed, 10% (5% goal). However, the inter-channel radiometric accuracy between the VNS channels is required to be better than 1%. This last requirement could not be achieved by "standard" radiometric calibration methods and a calibration method was developed using the VNS camera itself in collaboration with an integrating sphere that was used in radiance and irradiance modes.

After finalisation of the performance testing and calibration measurements the VNS camera was delivered to SSTL mid 2017 for further integration on the MSI Optical Bench Module and alignment with the TIR camera and other MSI subsystems by SSTL.

Keywords: EarthCARE, Calibration, Verification testing, Straylight, Optical instrument, Earth Observation, Optical, Mechanical.

1. INTRODUCTION

The EarthCARE satellite mission objective is the observation of clouds and aerosols from low earth orbit. The key spatial context providing instrument within the payload suite of four instruments is the Multi-Spectral Imager (MSI) [1]. The MSI is intended to provide information on the horizontal variability of the atmospheric conditions and to identify e.g. Cloud type, textures, and temperature. It will form earth images at 500m Ground Sample Distance (GSD) over a swath width of 150km; it will image earth in seven spectral bands: one Visible, one Near-IR (NIR), two Short-Wave IR (SWIR) and three Thermal IR (TIR). The instrument comprises two optical modules:

- The Thermal IR (TIR) optical unit [5].
- The Visible-NIR-SWIR (VNS) optical unit [3].

The development of the overall MSI instrument has been reported earlier [6], [7].

Figure 1. Rendering of the MSI instrument optical units.

The VNS optical unit essentially is a radiometric imager with four spectral bands and consists of the following four assemblies:

- VNS Camera
- VNS SWIR-2 radiator
- VNS Calibration Mechanism Assembly (CMA)
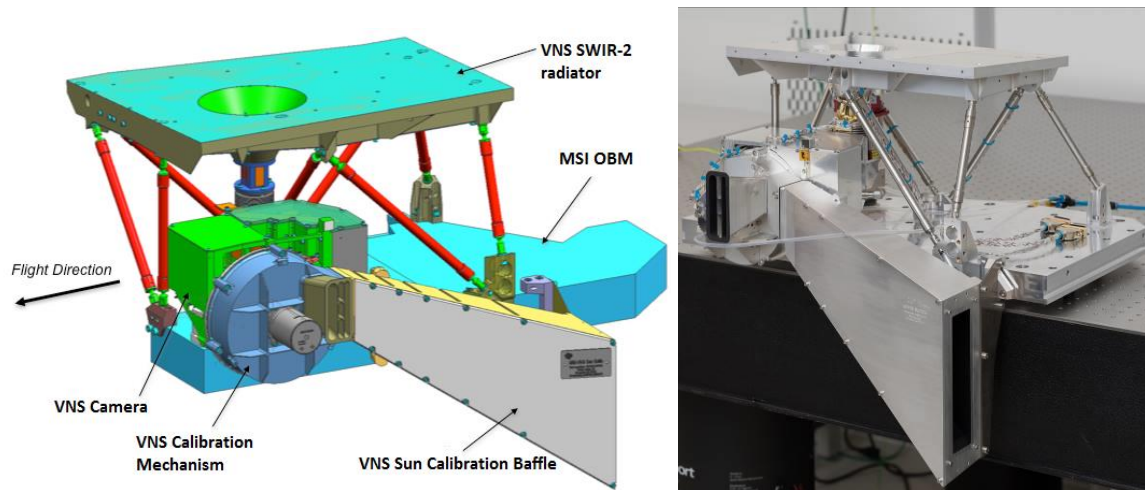- VNS Sun Calibration Baffle

Figure 2. CAD model of the VNSOU (left) and a the PFM model prior to delivery to SSTL (right)

The camera has two separate apertures (Figure 3), one for the VIS, NIR and SWIR-1 channels, and a second for the SWIR-2 channel.
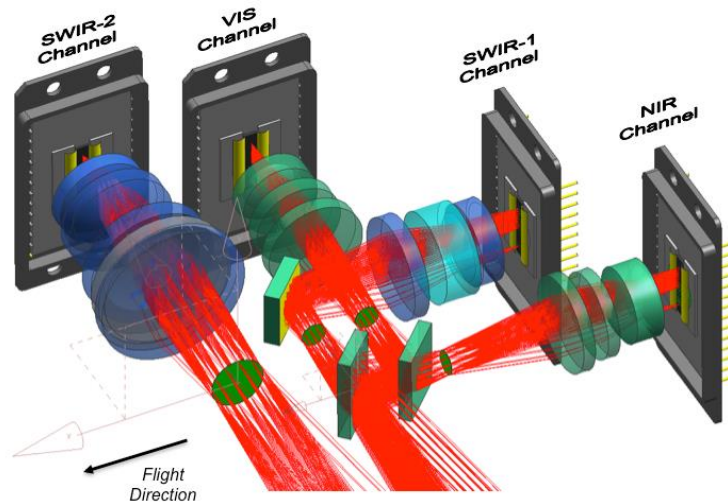

Figure 3. VNS camera optical configuration

The in-orbit operating temperature of the VIS/NIR and SWIR-1 detectors is 300K, while the operational temperature of SWIR-2 is 235K. The SWIR-2 radiator panel, with a surface of 0.175m2, is designed to allow to reach a temperature well below the target. An active thermal control circuit then stabilizes the SWIR-2 detector temperature at 235K.

In order to achieve the required radiometric accuracy of 10% absolute and 1% relative, the VNS will be regularly calibrated in-orbit. Two calibration points will be regularly obtained, a dark and a bright view. For the dark view the instrument aperture will be closed. For the bright view the sun light will illuminate one of two pairs of Quasi Volume Diffusers (QVD). One pair of daily QVDs are used by the two VNS apertures for a regular bright view every orbit, whilst occasional use of a monthly QVD pair will allow to monitor any degradation of the QVDs due to exposure. The QVDs are mounted on a rotating carousel (see Figure 4), which is used to switch between dark calibration, sun calibration and earth operational viewing modes.
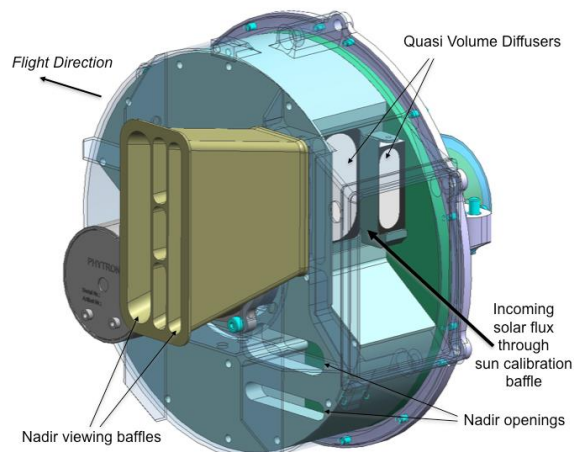
Figure 4. VNS Calibration mechanism

A Sun Calibration Baffle is implemented in order to prevent straylight during calibration. The baffle ensures that all reflections from the Spacecraft and the Earth are fully blocked.

In the rest of this paper the focus will be on the philosophy of the characterisation and performance verification (Chapter 2) of the VNS (including the SSTL Front End Electronics (FEE) Unit) and the execution of this philosophy on the VNSOU Proto Flight Model (PFM) (where R stands for refurbished) in chapter 3.

2. CHARACTERISATION AND PERFORMANCE VERIFICATION PHILOSOPHY

The overall VNS qualification and verification philosophy consisted of the development of several models:

- LifeTest Model (LTM)
  The purpose of this model was to qualify the VNS on-board calibration mechanism with respect to motorization margin and end of life performance. For this purpose a dedicated model was build and successfully tested. For more details reference is made to an earlier publication [9]

- Engineering Confidence Model (ECM)
  The purpose of the Engineering Confidence Model was to de-risk the development of the instrument, prior to the production of the Proto Flight Model (PFM). For this purpose a VNS ECM has been built with only two of the four spectral channels and exposed to the relevant environmental test. Additionally the two ECM channels were optically tested on performance and a dry-run of the characterisation (calibration) procedures was executed.

- Proto Flight Model (PFM)
  The final model in the development philosophy consisted of the Proto Flight Model. The aim of this model was to complete the qualification (with the exception of life test qualification), verify the complete instrument performance and to be fully characterized. After the achievement of these aims the PFM is ready to be integrated into the overall MSI instrument/EarthCARE satellite and to be launched for its 3 to 4 years in-orbit operation.

In order to achieve the goals of the PFM an overall test philosophy was setup consisting of environmental/IF tests (such as vibration, thermal, electrical and mechanical tests; outside of the scope of this paper) and optical tests (both in ambient and operational conditions) for characterisation and performance verification of the VNS PFM.

The optical tests were developed in order to determine the required Calibration Key Data (CKD), as part of the instrument characterisation, and to verify by test the optical performance (Optical Quality, Instrument Pointing, Spectral Performance and Straylight) in order to populate the Characterisation and Calibration DataBase (required as input for the instrument data processor, with parameters describing for instance the radiometric response function, pointing etc.).

3. CHARACTERISATION AND PERFORMANCE VERIFICATION OF THE VNS PFM

As described in the previous section the characterisation and performance verification of the VNS PFM consisted of the following tests that are described in more detail in in the rest of this chapter:

- OPTICAL QUALITY (MODULAR TRANSFER FUNCTION)
- POINTING AND CO-REGISTRATION
- SPECTRAL RESPONSE
- STRAYLIGHT
- RADIOMETRIC CHARACTERISATION

3.1 OPTICAL QUALITY (MODULAR TRANSFER FUNCTION)

The MTF performance was measured for each pixel of each channel for several spatial frequencies. The measurement was performed by scanning an illuminated block pattern in object space of the VNS camera's. For each pixel at least one period of the block pattern was recorded during a scan. Using Fourier analysis this signal was separated into its higher order components, resulting in the MTF performance for several sinusoidal spatial frequencies concurrently.

Theory

A square block function can be expressed as the infinite sum of sine functions:

$$f(x) = dc + \frac{4}{\pi}\sum_{k=1}^{\infty}\frac{\sin(2\pi(2k-1)fx)}{(2k-1)}$$

(1)

This spatial light distribution will be influenced by the MTF performance of the VNS instrument ($MTF_{VNS}(k)$), which will result in a VNS response of

$$S(x) = dc + \frac{4}{\pi}\sum_{k=1}^{\infty}\frac{\sin(2\pi(2k-1)fx)*MTF_{VNS}(k)}{(2k-1)}$$

(2)

By taking the Fast Fourier Transform of the VNS response, the amplitude ($A(k)$) for the base frequency f and its (2k-1) multiples can be obtained

$$A(k) = \frac{4}{\pi}*\frac{MTF_{VNS}(k)}{2k-1}$$

(3)

From these amplitudes the MTF performance for the embedded frequencies can be determined for each pixel

$$MTF_{VNS}(k) = \frac{\pi}{4}*(2k-1)*A(k)$$

(4)

MTF measurements have been carried out using block patterns with 20 lines/mm (Nyquist) in both flight (along track) direction and across flight direction. Therefore the sinusoidal MTF response can be analysed concurrently for 20 (k=1), 60 (k=2), 100 (k=3), etc. lines/mm from one measurement, where the signal of each pixel is recorded during a scan of one period or more. In across flight direction MTF measurement have also been carried out with a 10 lines/mm block pattern (resulting in simultaneous analysis results for 10, 30, 50, etc lines/mm).

MTF tool

In order to determine the MTF for a pixel the block pattern has to be scanned over that pixel for one period or more. To achieve this a dedicated MTF tool has been designed and built, it consists of a scanning object platform which can hold different reticles, which are illuminated by a line shaped white light source. The illuminated reticle is imaged at infinity by a folding mirror M1 and a collimating mirror M2. The folding mirror reduces the straylight level at the MTF tool exit

pupil position. The collimating mirror is split in two halves, to prevent light returning to the reticle that would affect the initial MTF value of the grating.

The reticle has several patterns of 5 x 110 mm in order to be able to measure different performance parameters of MSI. A block pattern of 1.8 lines/mm are used for MTF measurement in flight and across flight direction. Since the focal length of the MTF tool is about 11 times larger than the focal length of the MSI camera, the frequency of the imaged block pattern is 20 lines/mm. The object platform holding the reticle can be translated over a range of 10 mm in both flight and across flight direction independently with a resolution of 0.15 µm by means of stepper motors. The MTF measurements are performed with about 55 steps per period and using a scan length of at least 2 periods.
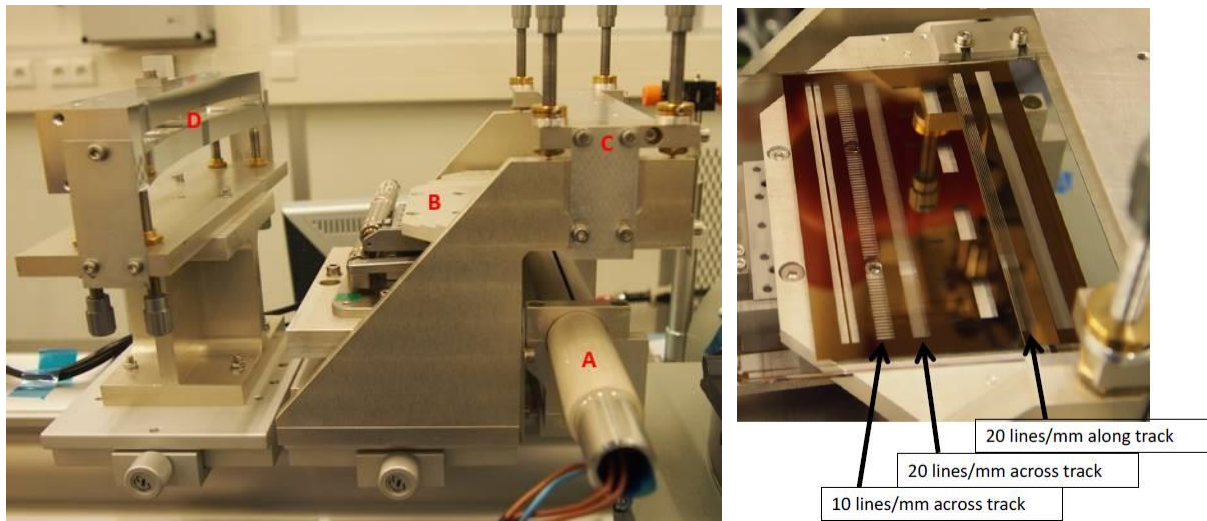

Figure 5. Left: MTF tool with light source (A), scanning platform (B), folding mirror (C) and collimating mirror (D)
Right: Reticle with different patterns

Results
The MTF performance has been measured with the VNS camera at operational conditions in a Thermal Vacuum setup. In this configuration the distance between the MTF tool and the VNS camera was about 1.3 m, which limited the MTF tool performance to an across flight field angle of about 1 degree. Therefore 25 measurements were performed to cover a total across flight field of view of 24 degrees. The presented results include predicted corrections for effects such as flight movement, spacecraft jitter, etc.

As can be seen the MTF performance of all the spectral channels (for the Nyquist frequency) is well above the required MTF performance of 0.25 (straight purple line in Figure 6) and confirms that the as build status of the VNS is in-line with the as designed status (and close to the nominal [without tolerances] expected performance).
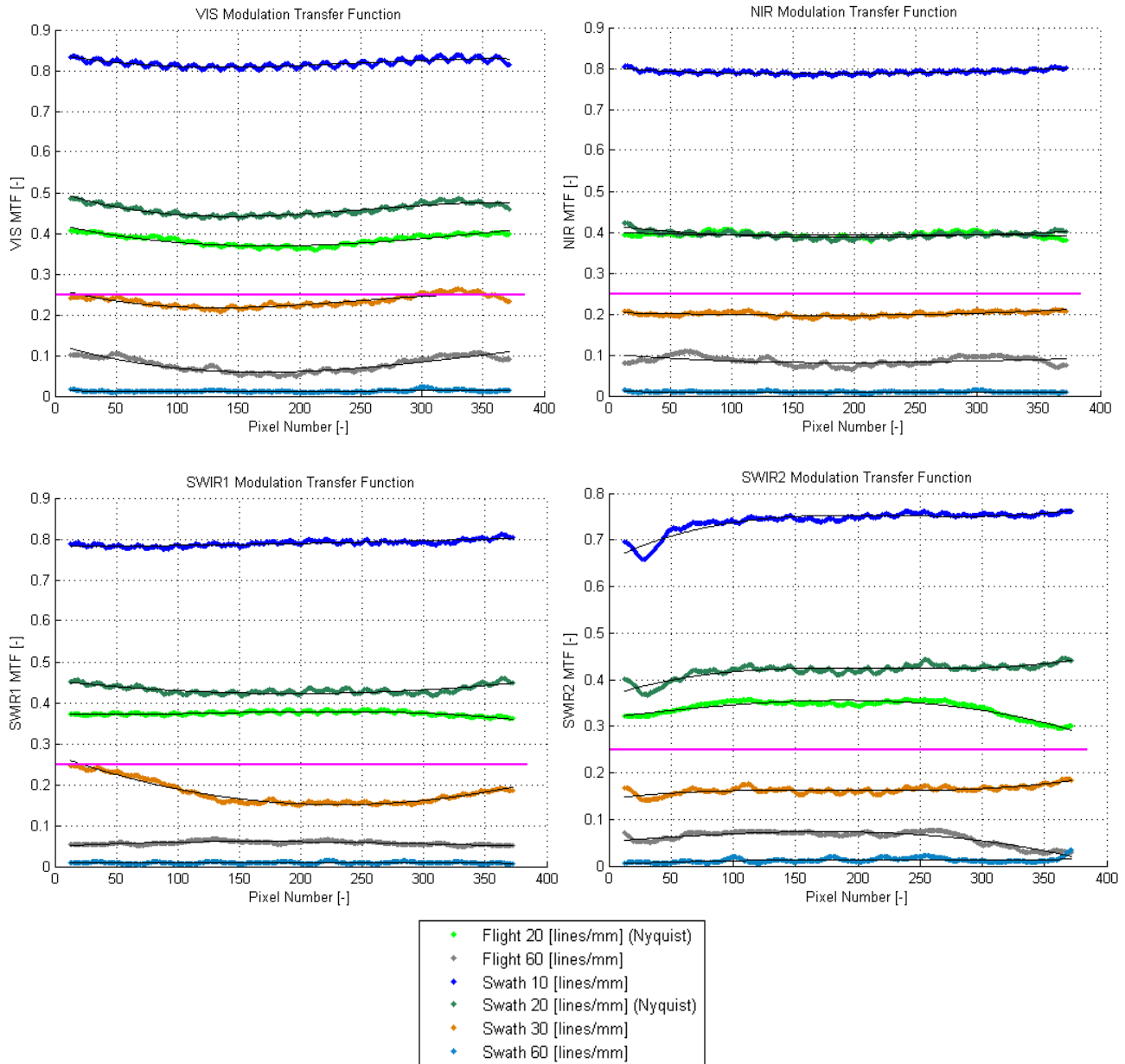
Figure 6. Measured MTF performance of the VIS (upper left), NIR (upper right), SWIR1 (lower left) and SWIR2 (lower right) camera in flight and across flight (swath) direction at several spatial frequencies. Note that the pink requirement line (@ 0.25) applies only to the Nyquist MTF.

3.2 SPECTRAL RESPONSE

The spectral response of the different channels within the VNS camera was measured over the wavelength range 300 to 2400 nm. Besides the spectral response within each channel, the setup is also used to measure the response when VNS was exposed to light outside the spectral bands of the VNS camera (out of band straylight).

Setup

Figure 3 shows the measurement setup with a tuneable laser (Ekspla NT242-SH) as light source. This laser provides nanosecond pulses with a 1 kHz repetition rate of which the wavelength can be tuned between 210 and 2600 nm. The laser beam was coupled via two mirrors into a 12 inch diameter integrating sphere in order to obtain an homogeneous

illumination over the full field of view of the VNS camera. The VNS camera was installed close to the 4 inch main opening of the sphere. A pyroelectric detector with an organic black coating and a flat response between 0.1 and 20 µm wavelength was mounted on one of the smaller output ports. This detector was used as reference detector to correct for the wavelength dependent output of the laser, reflection of mirrors and scattering of the sphere. Since the pyroelectric detector needs a modulated signal of a few hertz, a chopper operating at 4 Hz was installed in the laser beam.
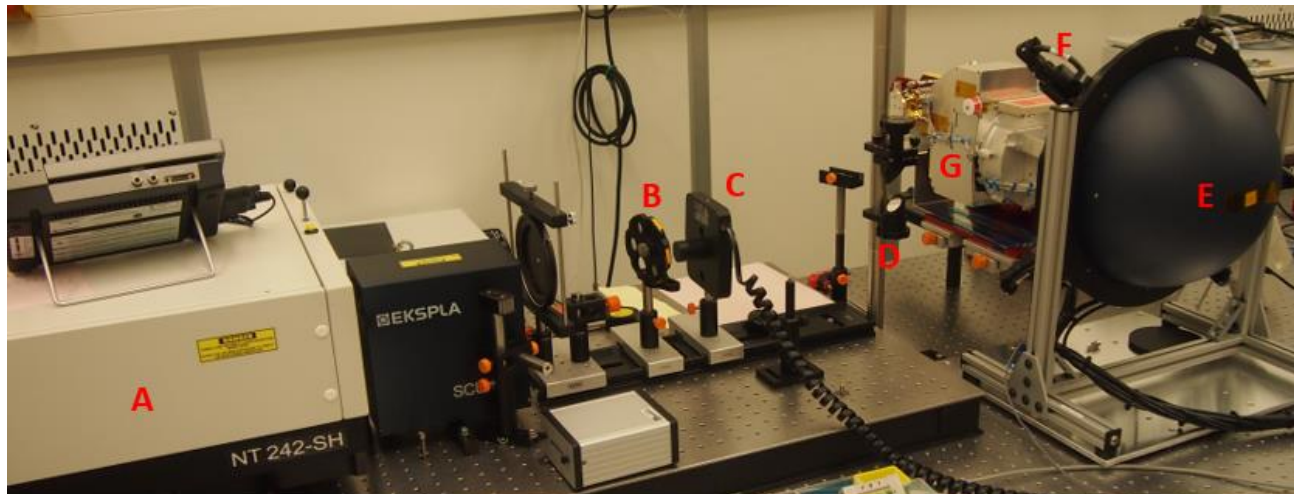

Figure 3. Spectral response test setup with tuneable laser (A), ND filter wheel (B) chopper (C), steering mirrors (D), integrating sphere (E) with reference detector (F) and VNS camera (G).

The measurements were performed in steps of 1 nm within the spectral band of each channel and in steps of 2 nm outside the spectral bands of the VNS camera. For each wavelength one or multiple samples of 75 s were recorded. The signal amplitude at 4 Hz was determined by taking a Fast Fourier Transform of each sample. Dark current correction was performed using the recorded signal on the so called wing pixels. These pixels are at both ends of the multi-element detector in each channel and are not illuminated because they are outside the clear aperture of the detector cover. Next the data was corrected for the wavelength dependency of the test setup using the reference detector data and converted to photons. In wavelength regions with relative low output power of the tuneable laser, up to 16 samples were taken and results are averaged after analysis, in order to reduce the measurement uncertainty.

Results

From the measurements the following output is extracted:

- Spectral response of each pixel for all channels

- Central wavelength of each pixel within a channel

- Out-of-band rejection

The spectral response for the central pixel in each channel is shown in Figure 4. The response is normalised in order to check if the response is within the required boundaries, which are represented by the red lines in Figure 4.
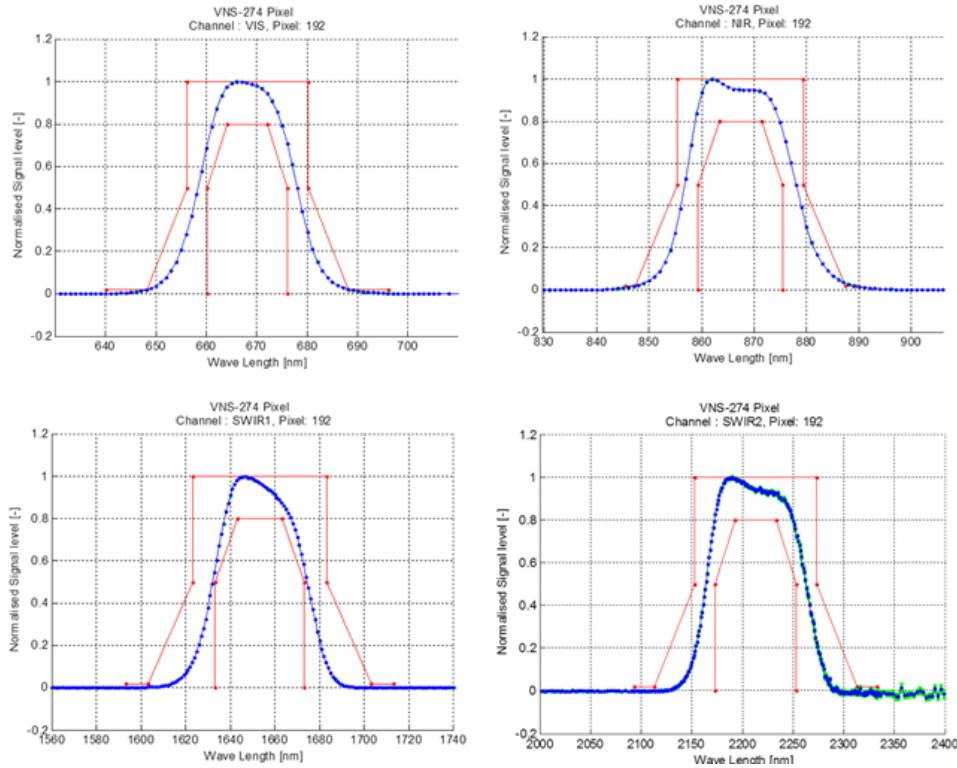
Figure 4. In-band spectral response requirement (red) and measured results (blue) for the central pixel of the VIS, NIR and SWIR channels of the VNS camera.

Figure 5 shows the normalised spectral response of the VIS and SWIR2 channel over the full wavelength range for which the detector in the corresponding channel is sensitive. This figure also shows the measurement uncertainty, which is generally well below 0.5% . Especially above 2200 nm the output of the tuneable laser is very low, leading to an increased measurement uncertainty of up to 2%. With the given light source further reduction of the measurement uncertainty in this wavelength region would lead to very long measurement times of over 1 month.

The central wavelength of the spectral response for a certain pixel is determined by the symmetry of the spectral response. Shift of the central wavelength over the VNS field of view should be minimised but may occur due to the performance of applied optical coatings. Figure 6 shows the two channels with the best (NIR) and worst (VIS) performance on central wavelength stability over the VNS field of view. Characterisation data for the change of central wavelength across the swath allows algorithms in the ground processor to reduce its effect in the processed imagery.

The out-of-band rejection (OOB) is defined as:

$$OOB = 1 - \frac{\int_{\lambda_{centee}-\Delta\lambda}^{\lambda_{centee}+\Delta\lambda} L(\lambda)R(\lambda)d\lambda}{\int_{0.3\,\mu m}^{20\,\mu m} L(\lambda)R(\lambda)d\lambda}$$

(5)

where R(λ) is the instrument spectral response and L(λ) is the spectral radiance of a source which simulates the solar spectral energy distribution (5820 K).
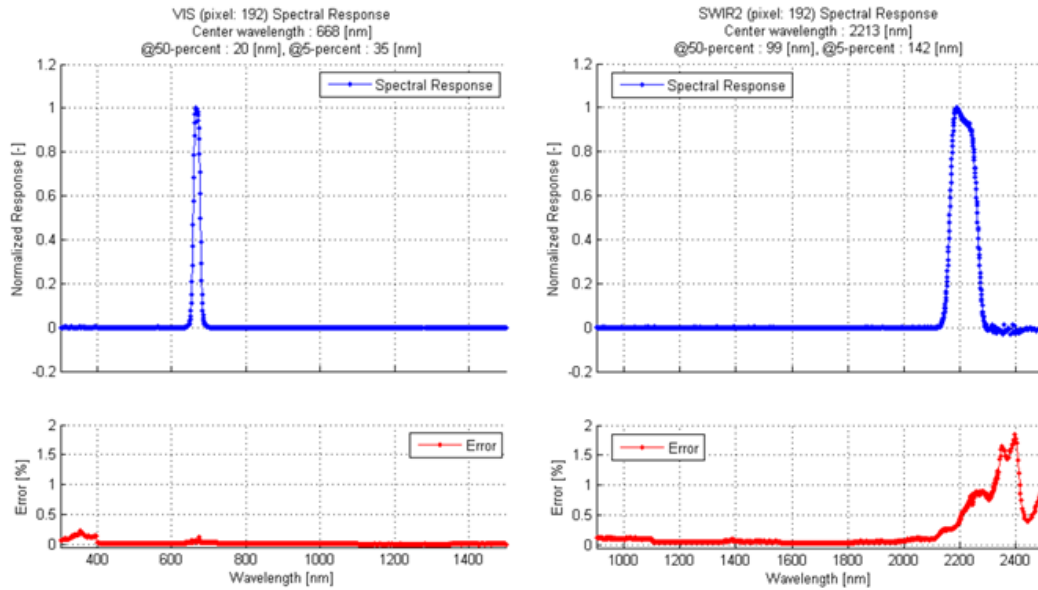
Figure 5. Spectral response of the VIS and SWIR2 channel (blue) and measurement uncertainty (red) over the full detector sensitive wavelength range of the corresponding channel.
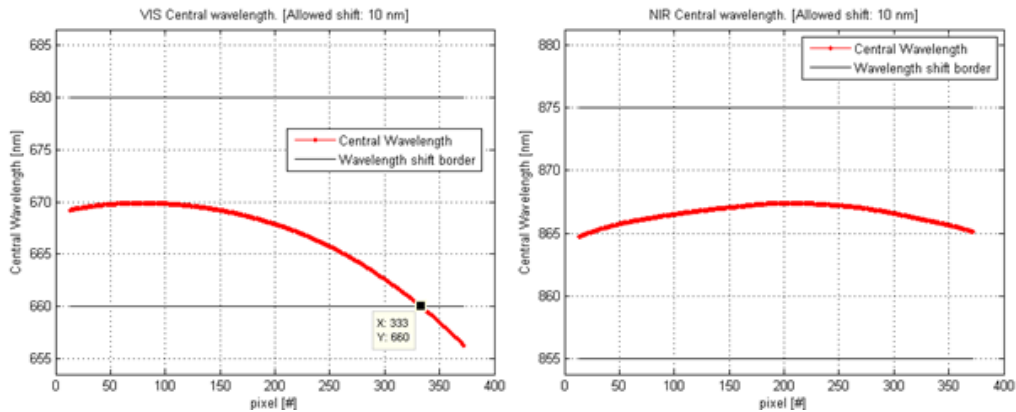

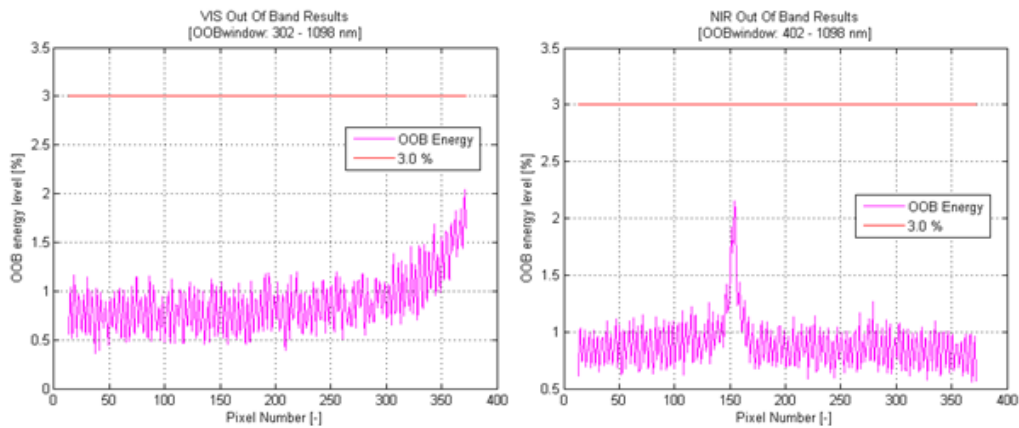Figure 6. Measured central wavelength over VNS field of view for the VIS (left) and NIR (right) channel.

Figure 7. Out-of-band rejection of the VIS (left) and NIR (right) channel.

The total integrated energy has been measured between 0.3 and 2.6 µm since none of the VNS detectors is sensitive to radiation above 2.6 µm. The measured out-of-band rejection was found to be mostly below 1% and always below 3%. Figure 7 shows the out-of-band rejection for the VIS and NIR channel.

Based on the measured spectral performances it was concluded that the VNS instrument fulfilled the specified requirements.

3.3 STRAYLIGHT

The straylight requirements for the VNS camera are specified as the maximum allowable amount of signal in an infinite dark area when illuminating the VNS camera with an adjacent semi-infinite bright area at a certain distance.

Setup

The straylight measurements are performed with the MTF tool described in section 3.1. In this case the scanning object platform holds a black coated mask to generate the step function scene with a bright illuminated and dark area, see Figure 7. Measurements were performed for both along track and across track directions. For along track measurements the mask is orientated such that the step function scene is in along track direction (see Figure 7). During these measurements the step function scene is moving along track with respect to the line of sight of the VNS camera; either towards the bright area (edge up) or away from the bright area (edge down). For across track measurements the mask is rotated 90 degrees rotated, resulting in the bright area being either left or right with respect to the track (flight) direction. During these measurements the step function scene is moving across track. The raw data obtained from the straylight measurements was dark level corrected and normalised on the maximum signal level; obtained when the pixel was fully illuminated by the bright area of the step function scene.
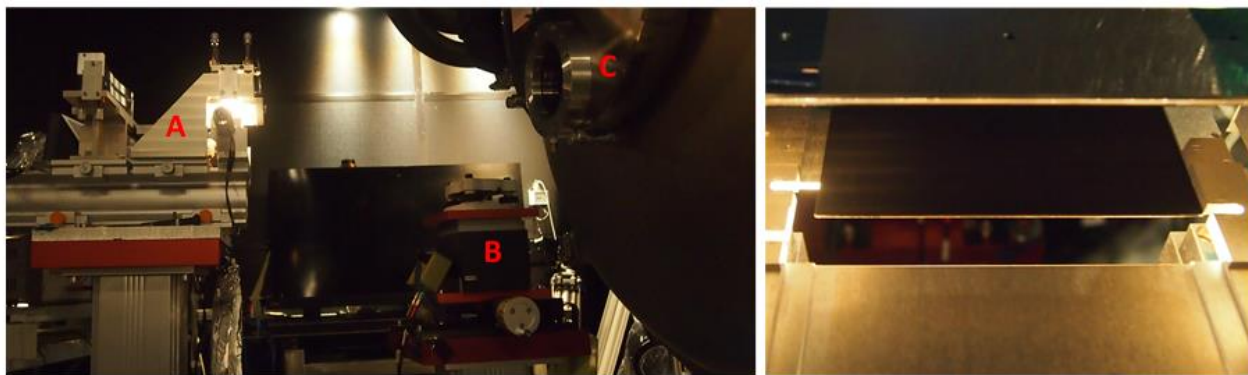

Figure 7. Straylight test setup with MTF tool (A), theodolite base (B) and entrance port of TV facility (C) with the VNS camera inside. At the right the object plane of the MTF tool with a black coated mask to generate the step function scene with a bright and a dark area along track.

Results

Figure 8 shows the detector response for pixel 195 of the SWIR1 channel during along track scans. The orange line is plotted where the normalised signal is 0.5, representing the condition where the border between dark and bright area is at the line-of-sight of the pixel. The straylight requirement is defined for the condition where the step function to the bright area is at a distance of 2.5 pixels at detector level. This condition is represented by the green line when the bright area is moving towards the pixel line-of-sight (MSI flying into bright area) and a blue line when the bright area is moving away from the pixel line-of-sight (MSI flying away from a bright area). In this case the amount of straylight is respectively 0.66% and 1.45%. Figure 9 shows these straylight results for 23 pixels distributed over the total field of view of the SWIR1 channel of the VNS camera.

Table 1 gives an overview of the measured straylight results for the different VNS channels at different conditions. These results include diffraction effects present in the measurement setup. Most straylight levels are around 1% which was the goal excluding diffraction effects, except for the SWIR2 channel. With the achieved straylight measurement results it was demonstrated that the VNS instrument is capable of fulfilling its overall performance requirements.
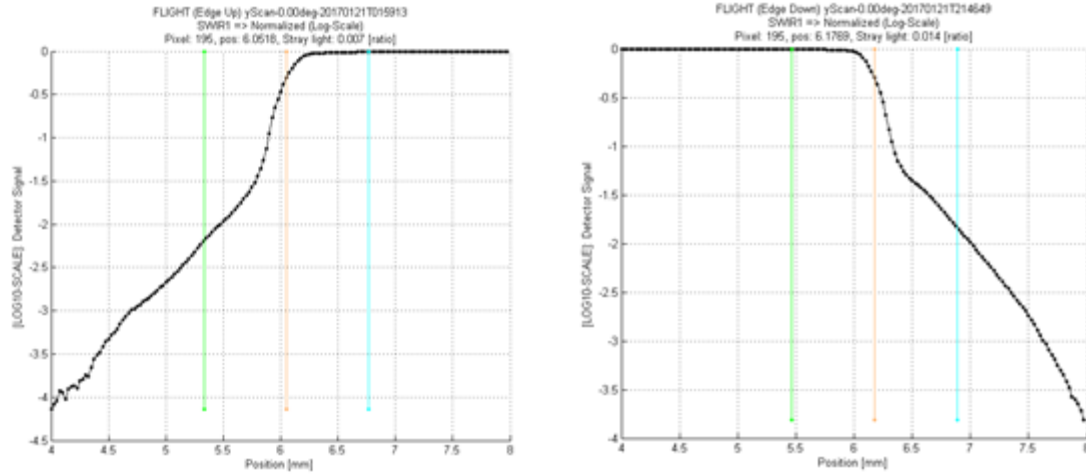
Figure 8. Detector response of pixel 195 of the SWIR1 channel (on log scale) when scanning towards a bright area (left) and away from a bright area (right). See text for explanation of the green, orange and blue lines.
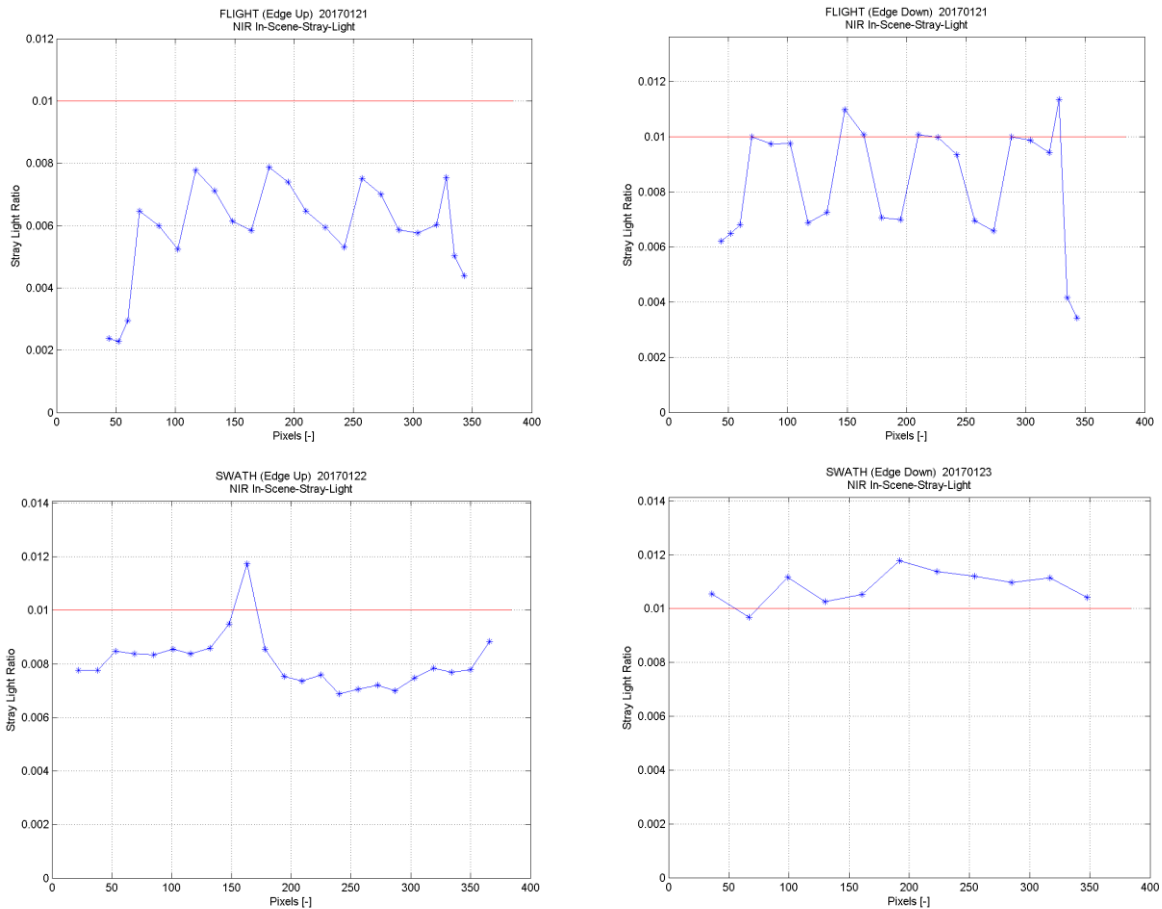

Figure 9. Measured straylight level for 23 pixels distributed over the field of view of the NIR channel, when MSI is flying towards a bright area (upper left), away from a bright area (upper right) or with a bright area left or right from the pixel line-of-sight (below).

Table 1. Straylight levels for different channels in the VNS camera and for different conditions (see text).

Channel	Along Track		Across Track	
	Bright area front	Bright area back	Bright area left	Bright area right
VIS	0.006	0.009	0.009	0.013
NIR	0.008	0.010	0.009	0.012
SWIR1	0.007	0.016	0.014	0.015
SWIR2	0.020	0.010	0.025	0.030

3.4 RADIOMETRIC CHARACTERISATION

The radiometric characterisation are the set of measurements necessary to determine the calibration key data necessary to transform the digital signal generated by the instrument into the radiance levels received by the instrument. This transformation is part of the Level 0 to Level 1B data processor.

- MSI Level-0: Raw instrument output [Digital Units]

- MSI Level-1b: Top Of Atmosphere radiances for four solar channels [Photons/s/nm/cm^2/sr]

Theory

In *Figure 10* a schematic representation of the MSI-VNS instrument is depicted. In the figure all relevant conversions that take place between receiving the TOA radiance and generating the instrument RAW data are described.
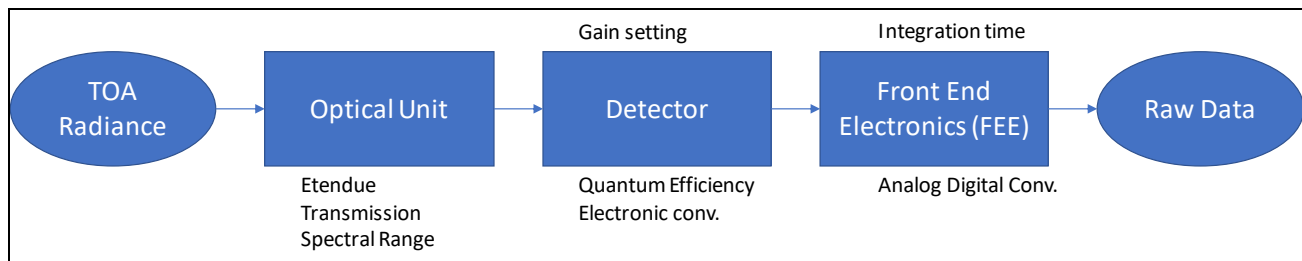

Figure 10. Schematic representation of the MSI-VNS optical unit including SSTL FEE. Above the detector and FEE box the settings of the unit that can be modified in flight are indicated. Below each box the parameters that influence the conversion are indicated.

For the data processor to reverse the conversions present in the VNS instrument (in order to go from Level-0 to Level-1B data), the conversion factor(s) needs to be determined during the radiometric characterisation.

The detail with which the conversion factors are determined can be (to a certain extent) freely chosen. The options here can be roughly divided in three approaches:

- *Determine each and every conversion factor separately.*
  This approach most accurately follows the physical transformations present in the instrument, but cannot be executed at instrument level only. This limitation is due to the fact that the optical measurements performed on the instrument itself cannot distinguish between detector electronics conversion, ADC conversion, Etendue, Transmission etc. This approach therefore heavily relies on sub-system and component level characterisation and measurements.

- *Separate the conversion factors that cannot be actively changed from the ones that can be actively changed.*
  In this approach all conversion factors that cannot be controlled (e.g. Etendue, Transmission, QE) are put in a single conversion factor or CKD. All other conversion factors will be determined separately (separate CKD) for each of their settings (for example the electronics conversion factor of the detector should be determined for the two different settings). This approach results in a flexible system were the Gain and integration time can relatively easily be modified during operations at the cost of some complexity during instrument level characterisation.

- *A single conversion factor for the instrument.*
  In this approach a single conversion factor is determined for the entire instrument combining all separate conversion factors. This approach is the most simple for the data processor at the cost of flexibility, as it is in reality not possible to measure the "single" conversion factor for each and every combination in settings. Therefore this approach results usually in the measurement of the conversion factor for several combinations of settings, were one is choosen as operational baseline and the rest are used to recalculate the baseline in case the settings need to be modified during operations in-orbit.

For MSI-VNS it was decided (together with the customer chain) to follow the single conversion factor approach. For MSI-VNS the lower flexibility was deemed acceptable because the in-orbit sun calibration system could be used to determine/measure in-orbit a correction factor in case the instrument settings required an update.

Note that the characterisation of the in-orbit sun calibration system is outside of the scope of this paper.

Setup

In order to determine the radiometric CKD a measurement setup needed to be developed that is capable of illuminating the instrument with a known (to within a few percent) radiance level. Additionally the radiance levels between the different spectral bands of the instrument required a 1% relative accuracy.

As the instrument, and especially detector temperature, have a significant influence on the radiometric responsivity of the system, it was required that the instrument was located in a thermal vacuum chamber and controlled to operational temperatures.
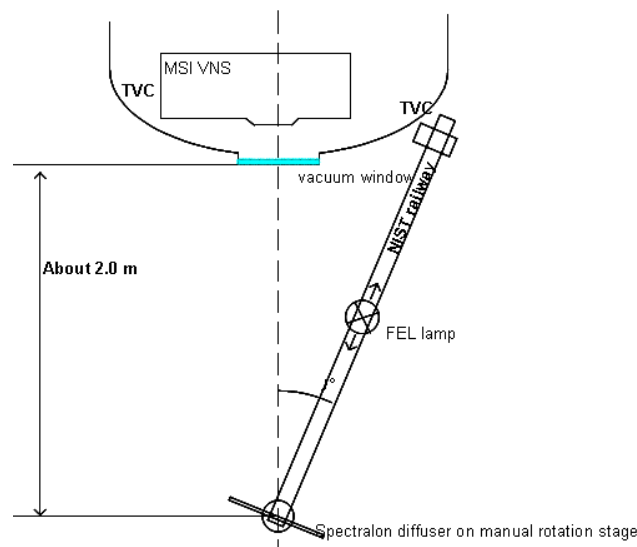

Figure 11. Setup for Radiometric Characterisation

The setup that was used consisted of a Finite Element Lamp (FEL; calibrated by the National Institute of Standards and Technology [NIST]) and a Spectralon diffuser. Although this setup seems quite simple the pain, is as usual in the details. The FEL lamp for example has a calibrated (to several tenths %) irradiance level that is only valid at 500mm distance. Any deviation from this distance directly results in additional errors; a 1mm alignment error results in an unacceptable error of 0.4%. So, during the characterization execution the distance between the FEL lamp and the diffuser was aligned to within 50µm. Due to the same effect only a small part of the surface of the flat spectralon diffuser could be used for accurate calibration purposes (the edges of the diffuser are further away from the lamp than the center).

Aside from all the apparent critical alignment error contributions in the setup, also the BRDF of the Spectralon diffuser needed to be known accurately (both absolute and relative between the four VNS channels) in order to execute a conversion from lamp irradiance levels to radiance levels. Based on a market research (in 2011) into the achievable calibration accuracies for this diffuser it was found that, especially for the SWIR (short wave infrared), the accuracy was lacking. The highest accuracy that could be found at institutes worldwide was ~1.2%. Although this accuracy was just acceptable for the absolute calibration of the instrument, it was insufficient for the 1% relative accuracy between the

different instrument bands. In order to remedy this lacking accuracy a measurement was setup to use the VNS to calibrate the Spectralon diffuser.

The dedicated Spectralon diffuser calibration procedure consisted of two steps:

1. A measurement where the VNS instrument directly observes the radiance of an integrated sphere. The instrument directly looks into the integrating sphere (*Figure 12*). Resulting in the following measurement signal

$$S_{VNS\_SP\_Direct} = L_{Sp} * T_{VNS}$$

(5)

In this formula

$S_{VNS\_SP\_Direct}$ is the signal level in binary units generated by the instrument
L_{sp} is the radiance level generated by the integrating sphere
T_{VNS} is the instrument response function

2. A measurement where the VNS instrument observes the radiance levels coming from the Spectralon diffuser, while the diffuser is illuminated by the integrating sphere. (*Figure 13*). Resulting in the following measurement signal (based on the Walker approximation to convert the irradiance levels of a integrating sphere in radiance levels)

$$S_{VNS\_SP\_RAD} = \frac{\pi * r_{sp}^2}{d_{sp}^2 + r_{sp}^2 + R_{Det}^2} * L_{Sp} * BSDF_{Spectralon} * T_{VNS}$$

(6)

In this formula the additional parameters are

$S_{VNS\_SP\_RAD}$ is the signal level in binary units generated by the instrument
r_{sp} is the radius of the sphere exit aperture
d_{sp} is the distance between the sphere exit aperture and the spectralon diffuser
R_{Det} is the footprint on the diffuser that is observed by the VNS instrument
$BSDF_{Spectralon}$ is the Bi-directional scatering function of the Spectralon diffuser

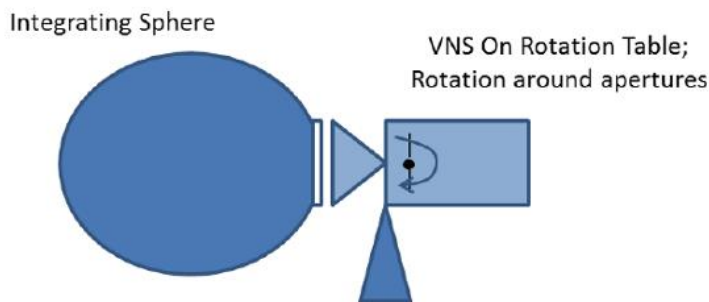In Figure 14 a picture of the used setup is visible.
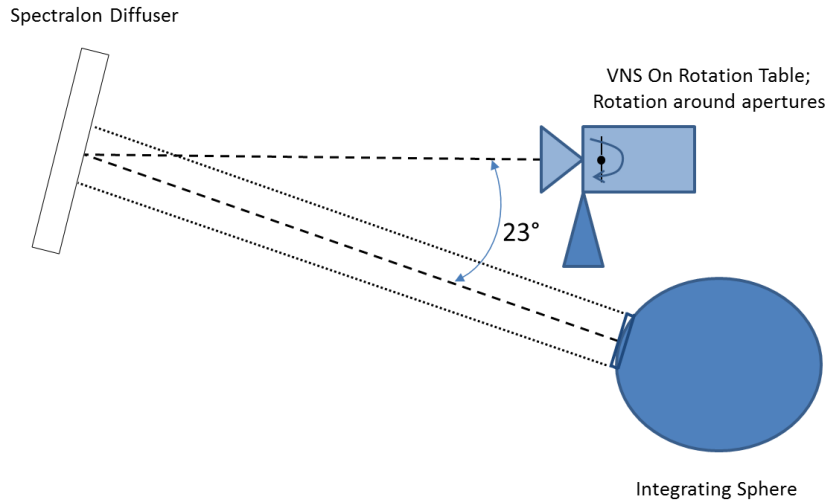

Figure 12. Direct sphere measurement setup

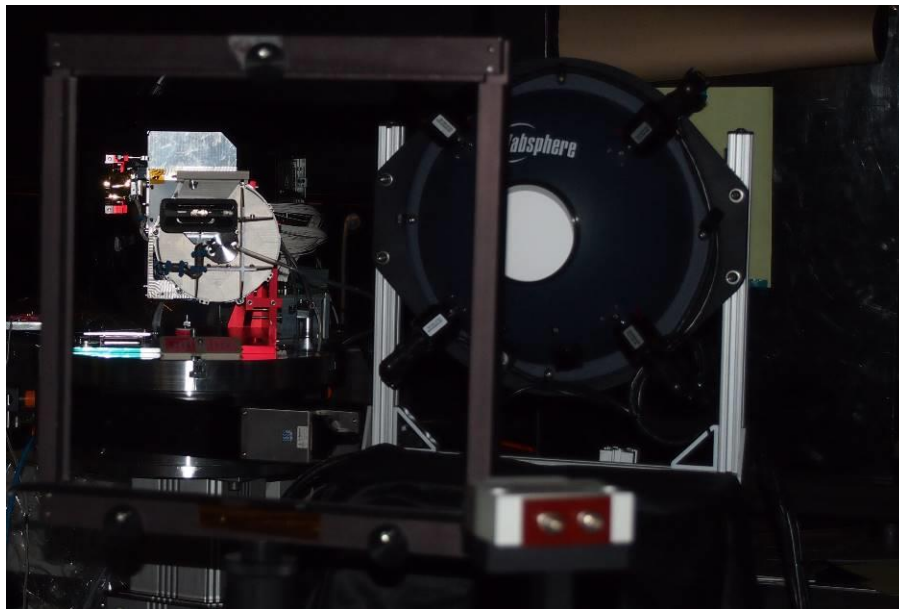Figure 13. Sphere over diffuser measurement setup

Figure 14. Photo of sphere over diffuser setup. On the left in the picture the VNS Optical unit is visible through the mounting frame of the Spectralon diffuser, on the right the integrating sphere is visible.

By combining the result of equation 5 and 6 the BSDF of the diffuser can be extracted

$$BSDF_{Spectralon} = \frac{S_{VNS\_SP\_RAD}}{S_{VNS\_SP\_Direct}} * \frac{d_{sp}^2 + r_{sp}^2 + R_{Det}^2}{\pi * r_{sp}^2}$$

(7)

Using this approach, the BSDF of the spectralon diffuser could be determined with a 1.9% absolute accuracy and a 0.65% relative accuracy, resulting in an overall slight reduction of absolute accuracy but a significant gain in relative accuracy. By implementing this approach the overall instrument requirements for radiometric accuracy, could be achieved.

Results

Using the described setup the radiometric conversion factor (or CKD) for each pixel of the four VNS channels was determined. The results of these measurements are depicted in *Figure 15*.

Based on these results 2 specific items can be pointed out:

1. It was expected that the instrument responsivity would decrease towards the edges of the instrument Field of View, which is clearly visible in the VIS and NIR channel and to a lesser extend in the SWIR-2 channel. The SWIR-1 channel is not following this expectation and an investigation into this effect demonstrated that the behavior observed in the SWIR-1 channel can be explained by the interaction of a small change of the central wavelength over the FoV (at the edge the observed wavelength is slightly lower than in the center) and the spectral quantum efficiency of the used InGaAs detector (QE increases slightly for lower wavelengths).

2. In both the VIS and SWIR-1 (and to a lesser extent the SWIR-2) it is clearly visible that the responsivity of the odd and even pixels is different in the detector. This behavior was expected due to the design of the detector, where the odd pixels are read-out though one amplifier and the even though another amplifier. Small differences in the gain between the two amplifier / read-out chains results in the difference in responsivity between the odd and even pixels.
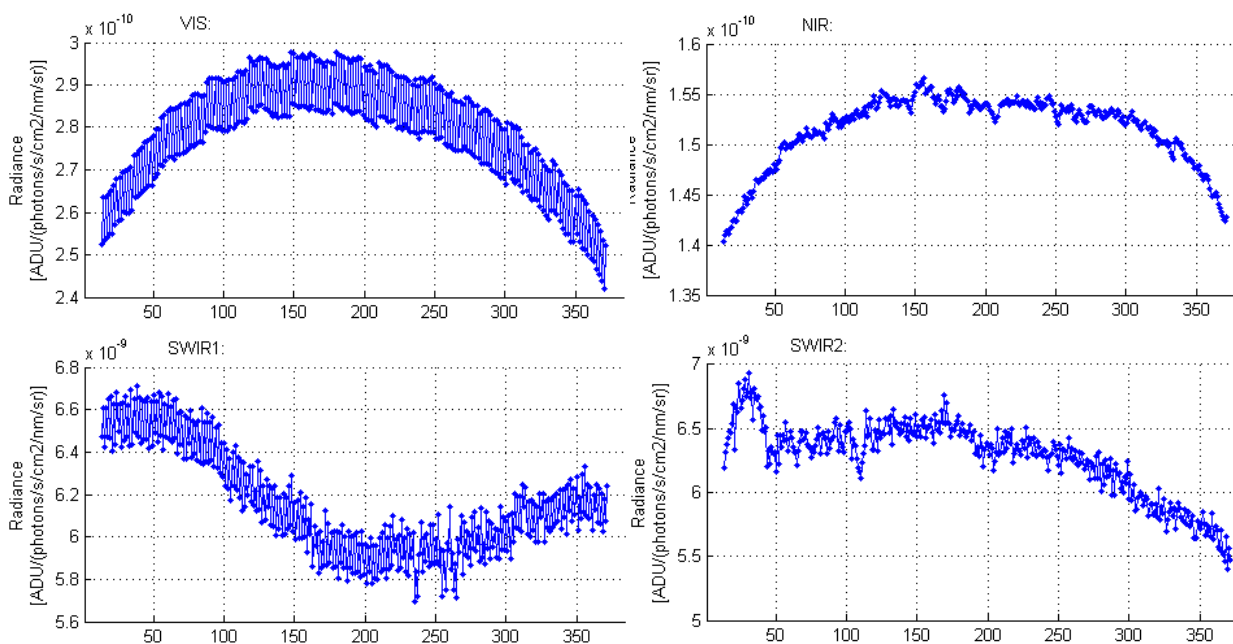

Figure 15. Determined Radiometric Response CKD values for each pixel and each VNS channel.

The achieved characterisation error for these measurements is 1.98% absolute and ~0.95% relative between each VNS channel. With these accuracies the overall VNS instrument performance is guaranteed and the instrument requirements are achieved.

4. CONCLUSION

Characterization and Performance Verification of the VNS instrument took place after successfully passing the environmental tests in the timeframe August 2016 – April 2017. The Post Test Review took place early May 2017 after which the VNS Instrument was shipped to SSTL for further integration with the TIR camera module. The characterization and verification of the PFM VNS has been done and the results show that the instrument performance is within the requirements. New calibration strategies have been followed and have been demonstrated to be viable.

REFERENCES

[1] D. Lobb, I. Escudero Sanz, M. Chang and S. Gode, "Development of Detailed Design Concepts for the EarthCARE Multi-Spectral Imager" in proceedings of the International Conference on Space Optics, October 2008.

[2] A. Pérez Albiñana, R. Gelsthorpe, A. Lefebvre, M. Sauer, E. Weih, K-W. Kruse, R. Münzenmayer, G. Baister, M. Chang, "The multi-spectral imager on board the EarthCARE spacecraft", Proc. SPIE 7808, 780815 (2010); http://dx.doi.org/10.1117/12.858864

[3] J. Doornink, B. de Goeij, O. Marinescu, E. Meijer, R. Vink, W. Van Werkhoven, A. van 't Hof, "The Visible, Near-Infrared and Short Wave Infrared Channels of the EarthCARE Multi-Spectral Imager" in proceedings of the International Conference on Space Optics, October 2010

[4] M. P. J. L. Chang, D. Woods, G. Baister, D. Lobb, T. Wood, "The EarthCARE Multi Spectral Imager Thermal Infrared Optical Unit" in proceedings of the International Conference on Space Optics, October 2010

[5] L. Gomez Rojas, M. Chang, G. Baister, G. Hopkinson, M. Maher, M. Price, M. Skipper, T. Wood, D. Woods, "The EarthCARE multispectral imager thermal infrared optical unit detection system design", Proc. SPIE 7826, 7826H (2010); http://dx.doi.org/10.1117/12.869250

[6] M. Chang, B de Goeij, et all "Overview of the EarthCARE Multi-Spectral Imager and Results from the Development of the MSI Engineering Model", in proceedings of the International Conference on Space Optics, October 2012.

[7] Abelardo Pérez-Albiñana ; Robert Gelsthorpe ; Alain Lefebvre ; Maximilian Sauer ; Klaus-Werner Kruse ; Ralf Münzenmayer ; Guy Baister ; Mark Chang ; Julie Everett ; Andy Barnes ; Nigel Bates ; Matt Price ; Mark Skipper ; Bryan T. G. de Goeij ; Ellart A. Meijer ; Frits van der Knaap ; Adriaan Van't Hof; "The engineering model for the multispectral imager of the EarthCARE spacecraft", Proc. SPIE 8511, Infrared Remote Sensing and Instrumentation XX, 85110L (October 24, 2012); doi:10.1117/12.928912

[8] A.Helière, K. Wallace, J. Pereira do Carmo, M.Eisinger, T.Wehr, A.Lefebvre; "EarthCARE instruments description, EC-TN-ESA-SYS-0891"; 24/05/2017.

[9] Bryan de Goeij, Erik Tabak, Luud van Riel, Ellart Meijer, Frits van der Knaap, Jan Doornink, Harm-Jan de Graaf; "DESIGN, BUILDING AND TESTING OF A SUN CALIBRATION MECHANISM FOR THE MSI-VNS INSTRUMENT ON EARTHCARE"; ESMATS 2013